

Journal of Materials Chemistry A

Accepted Manuscript

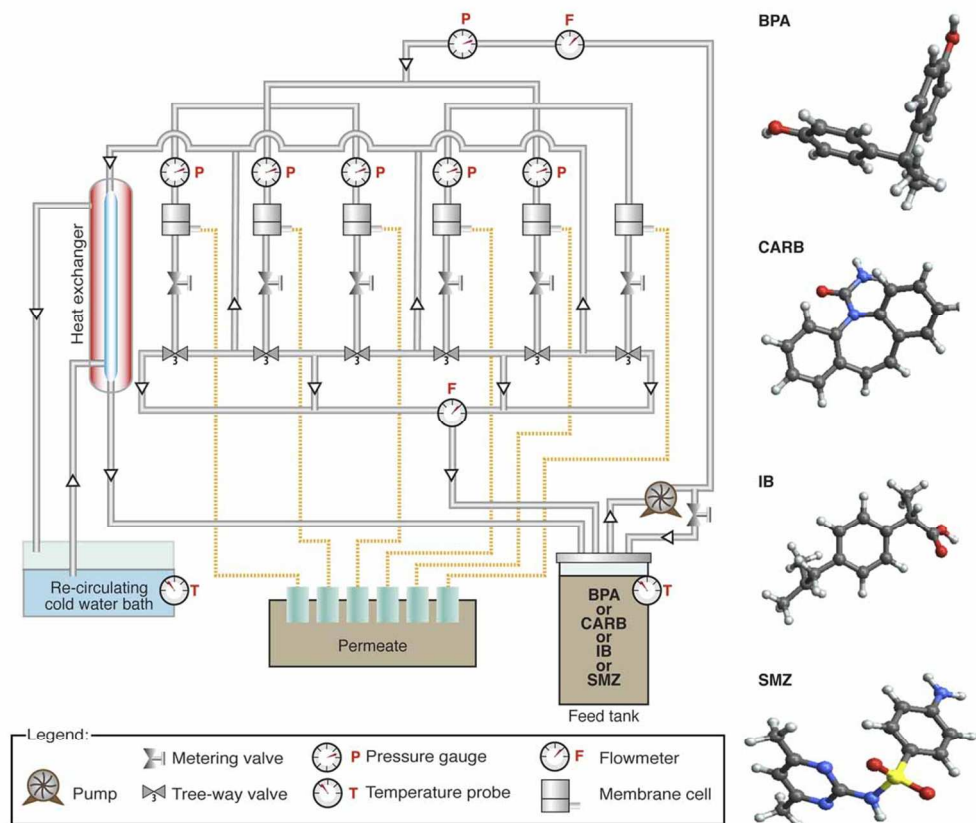


This is an *Accepted Manuscript*, which has been through the Royal Society of Chemistry peer review process and has been accepted for publication.

Accepted Manuscripts are published online shortly after acceptance, before technical editing, formatting and proof reading. Using this free service, authors can make their results available to the community, in citable form, before we publish the edited article. We will replace this *Accepted Manuscript* with the edited and formatted *Advance Article* as soon as it is available.

You can find more information about *Accepted Manuscripts* in the [Information for Authors](#).

Please note that technical editing may introduce minor changes to the text and/or graphics, which may alter content. The journal's standard [Terms & Conditions](#) and the [Ethical guidelines](#) still apply. In no event shall the Royal Society of Chemistry be held responsible for any errors or omissions in this *Accepted Manuscript* or any consequences arising from the use of any information it contains.



Graphical Abstract
210x177mm (150 x 150 DPI)

Development of novel charged surface modifying macromolecules blended PES membranes to remove EDC and PPCPs from drinking water sources

Cite this: DOI: 10.1039/x0xx00000x

Received 00th March 2014,
Accepted 00th xxxx 2014

DOI: 10.1039/x0xx00000x

www.rsc.org/

Dipak Rana ^{a,*}, Roberto M. Narbaitz ^b, Anne-Marie Garand-Sheridan ^{b,†},
Amy Westgate ^{b,†}, Takeshi Matsuura ^a, Shahram Tabe ^c and Saad Y. Jasim ^{d,‡}

The aim of this study was to develop novel surface-modified poly(ether sulfone) (PES) ultra-filtration (UF) membranes for removal of endocrine disrupting chemicals (EDCs) and pharmaceutical and personal care products (PPCPs). Seven tailor-made charged surface modifying macromolecules (CSMMs) were developed to use as additives in the preparation of PES UF membranes with a greater surface charge and improved PPCPs and EDCs removals through charge repulsion. Twenty three types of PES membranes were prepared using two amounts of different CSMMs and two drying (or evaporation) times. The experiments were designed to obtain the membranes' performances in terms of normalized standard flux (NSF), molecular weight cut-off (MWCO), surface charge (SC), static contact angle and their removal efficiency towards one EDC (bisphenol A) and three PPCPs (carbamazepine, ibuprofen, and sulfamethazine). The correlation between NSF versus SC, MWCO, pore density, and porosity was discussed. The filtration experiments showed an initial partial removal of the target compounds, but no removal in the later stages of operation, which indicated that charge repulsion was not the controlling removal mechanism. This is consistent with low changes in membrane surface charge achieved by addition of these additives. Given the decrease in the percent removals with time, removal by size exclusion was also not significant as expected because the membranes had a MWCO greater than 10 kilo-Dalton while the target compounds had molecular weights in the 200 to 300 Dalton range. Based on the decreasing level of removal with time, it appeared adsorption was the main removal mechanism.

1. Introduction

Endocrine disrupting chemicals (EDCs), and pharmaceuticals and personal care products (PPCPs) are two groups of chemicals that have recently been detected in water sources.¹⁻⁶ The detection of these pollutants has raised concerns about their potential impacts on the environment and human health. EDCs and PPCPs comprise a very broad, diverse collection of thousands of chemical substances, including prescription and over-the-counter therapeutic drugs, fragrances, cosmetics, sun-screen agents, diagnostic agents, nutraceuticals, biopharmaceuticals, and many others. This broad collection of substances refers, in general, to any product consumed by individuals for personal health or cosmetic reasons. Large quantities of EDCs and PPCPs (and their metabolites) are used by multitudes of individuals or domestic animals, and are subsequently discharged to (and incompletely removed by) sewage treatment systems. EDC and PPCP residue in treated sewage effluent (or in terrestrial run-off or directly discharged raw sewage) then enter the environment, which creates a great environmental concern.⁷

Due to dilution and in-stream adsorption, settling, biodegradation and volatilization, the concentration of EDCs and PPCPs decreases in the receiving waters. The river flow rate and nature of the contamination source (urban versus agricultural sources), and continuous/intermittent discharges versus cumulative

effects, are the important factors controlling the relative frequency of detection and variability of different PPCPs in surface waters.⁵ In spite of this reduction in EDC and PPCP concentrations they are still detectable at PPT (ng/L) levels at water treatment plant intakes. Part of the concern arises from the inadequacy of conventional water and wastewater treatment processes in removal of these compounds.⁷⁻¹² Membranes can separate chemicals via sieving, charge repulsion, and adsorption. Briefly, removal by sieving mechanism occurs when the solutes are larger than the membrane pores and therefore, cannot pass through.¹³ Separation by charge repulsion mechanism arises when the electrostatic repulsive force between the charged membrane surface and the ions of electrolyte solutes prevents the ion from contacting the membrane.¹⁴ Even reverse osmosis (RO) membranes (having the smallest pores) remove many but not all low molecular weight organic compounds (such as EDCs and PPCPs) based primarily on the pore size. It has been demonstrated that certain EDCs and PPCPs can be removed by some nano-filtration (NF) membranes.¹⁵ Removal via adsorption occurs when contaminants adsorb onto the membrane material.

NF membranes are suitable for separation of solutes, having molecular weights as low as a few hundreds, from water at operating pressures ranging from 50 to 150 psig. The NF membranes are prepared by surface modification of a porous substrate by either

Paper

a) depositing a thin selective layer and conducting in-situ polymerization of the layer; or b) coating the porous substrate with a thin layer of polyelectrolyte. This surface modification involves an extra manufacturing step. NF membranes have pore sizes approximately equal to one nanometer and most are negatively charged. Based on operational costs, NF membranes are preferable to RO membranes due to their higher fluxes and lower operating pressures. For the same reasons, micro-filtration (MF) and ultra-filtration (UF) membranes would be preferable to NF membranes. However, most UF and MF membranes used at water treatment plants have rather large pores (molecular weight cut-off ≥ 10 kDa) and thus are unable to separate EDCs and PPCPs molecules via sieving. Tighter UF membranes could potentially remove certain PPCPs and EDCs.¹³

For the past 20 years, a part of the efforts in our group has been focused on improving membrane performance by developing tailor-made surface-modifying polymeric additives for ultrafiltration membranes.¹⁶⁻²⁰ The key features of these additives called Surface Modifying Macromolecules (SMMs) are that: a) they mix with the base polymer allowing the membrane to be prepared using a single casting step, as opposed to multi-step processing required for preparation of composite membranes; b) they are entrenched in the polymer matrix so they do not leach out, as do other additives; and c) after casting, they migrate to the surface of the membrane thus imparting different characteristics to the membrane. Our group has developed several hydrophobic and hydrophilic SMM additives. This led to the hypothesis that tailor-made Charged SMMs (CSMMs) could be developed and incorporated into tight ultrafiltration membranes in order to increase their charge and approach the performance of NF membranes for the removal of EDCs and PPCPs. In particular, the CSMMs with the end groups that contain aromatic rings with sulfonate groups can form complexes with EDC and PPCPs. More specifically, the CSMMs are end-capped by aromatic rings with sulfonate groups, it is then expected that the electron density of the aromatic ring decreases and the aromatic ring attracts EDC and PPCPs materials that contain electron donating functional group such as primary amine, carboxylic acid, amide and phenolic hydroxyl, by forming charge transfer complexes. Thus, blending of the CSMMs into the membrane may lead to stronger adsorption of EDC and PPCPs materials, particularly when their end-capping aromatic rings are projected outward at the membrane surface as a result of CSMM surface migration.

The objective of this research was to test this hypothesis by synthesizing several CSMMs, manufacturing PES UF membranes incorporating the CSMMs, and evaluating their removal of selected PPCPs in a cells-in-parallel membrane filtration system.

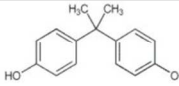
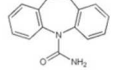
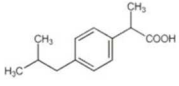
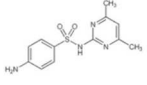
2. Experimental

Materials

Poly(ether sulfone) (PES) (Victrex 4100P, ICI Advanced Materials, Billingham, UK, average molecular weight ~ 17 -19 kDa) is used as the base polymer. The monomer 4,4'-methylene bis(phenyl isocyanate) (4,4'-diphenylmethane diisocyanate, MDI, purity 98%), used in the preparation of the CSMM additives, was purchased from Sigma-Aldrich Inc. (St. Louis, MO) and used without further purification. The solvents: *N,N*-dimethylacetamide (DMAc, anhydrous, 98%) and 1-methyl-2-pyrrolidone (*N*-methyl-2-pyrrolidone, NMP, +99.5%) were purchased from Sigma-Aldrich Inc. (St. Louis, MO). Poly(ethylene glycol) (PEG) of number average molecular weight (M_n) 200 Dalton to 35 kDa, and

poly(ethylene oxide) (PEO) of viscosity average molecular weight of 100 kDa, which were used in the solute testing, were supplied by Sigma-Aldrich Inc. (St. Louis, MO). Poly(propylene glycol) (PPG) of M_n 425 Dalton, diethylene glycol (DEG), sodium salt of hydroxyl benzene carboxylate (HBC), sodium salt of hydroxyl benzene sulfonate (HBS), disodium salt of 1-naphthol 3,6-disulfonate (NDS) and potassium chloride (KCl) were also purchased from Sigma-Aldrich Inc. (St. Louis, MO). Potassium hydroxide (KOH) and hydrochloric acid (HCl) were purchased from Fisher Scientific (Hampton, NH). Three compounds representing PPCPs (carbamazepine (CARB), ibuprofen (IB, $\geq 98\%$), and sulfamethazine (SMZ, $\geq 99\%$) and one EDC (bisphenol A (BPA, +99%)) were obtained from Sigma-Aldrich Inc. (St. Louis, MO). The physico-chemical properties and chemical structure of these compounds are summarized in Table 1. Reagent grade water was prepared by treating distilled water with Milli-Q water system (Millipore, Bedford, MA). The system incorporates mixed bed ion exchange resins, synthetic activated carbon, organic scavengers and membranes. This Milli-Q water was used to conduct membrane pre-compaction, conduct pure water filtration tests and prepare the solutions for the solute transport tests.

Table 1 Properties of selected EDC and PPCPs.

Compound	MW (g/mol)	Log K _{ow}	pK	Solubility (mg/L)	Structure
Bisphenol A (BPA)	228.29	3.32; 3.40 [†]		120-300 [†]	
Carbamazepine (CARB)	236.27	2.18 to 2.93	<2-2.45; 7	17.7, 18; Practically insoluble in water [†]	
Ibuprofen (IB)	206.28	3.14 to 4.5	4.4-4.9; 5.2	49; Relatively insoluble in water [†]	
Sulfamethazine (SMZ)	278.33	0.28	pK _{a1} = 7.4±0.2 pK _{a2} = 2.65±0.2 [†]	430; 1500 (29°C) [†] ; 1920 (37°C) [†] ; increases w/ pH [†]	

[†] Source: Ref. 21

Synthesis of charged surface modifying macromolecules (CSMMs)

Seven CSMMs were prepared using a two-step polymerization method,¹⁸ a schematic presentation of the CSMM is presented in Fig. 1. In the first step, a urethane prepolymer backbone was formed by reacting hard segment, i.e., MDI, with a di-ol (or soft-segment) in a solvent (DMAc). A number of different soft segments were used, including DEG, PEG (of M_n 200 and 400 Daltons), and PPG. The prepolymer is a segment-blocked urethane oligomer having both ends capped with isocyanate.

The second step involved end-capping the polymer with a number of different charged species (i.e., HBC, HBS and NDS). The reaction was then terminated by the addition of a reagent having a charged group on one-side and a hydroxy group on the other. The different mid-segments should impact the stiffness of the polymer and thus its ability to migrate to the surface. The CSMMs are named

Journal of Materials Chemistry A

Paper

by the acronym S-E, where S is the abbreviated name of the soft segment and E is the abbreviated name of the end-capping compound. So PPG-HBC was prepared using PPG as the soft segment and HBC as the end capping compound. The seven synthesized CSMMs are DEG-HBC, DEG-HBS, DEG-NDS, PEG₂₀₀-HBS, PEG₄₀₀-HBS, PPG-HBC, and PPG-HBS.

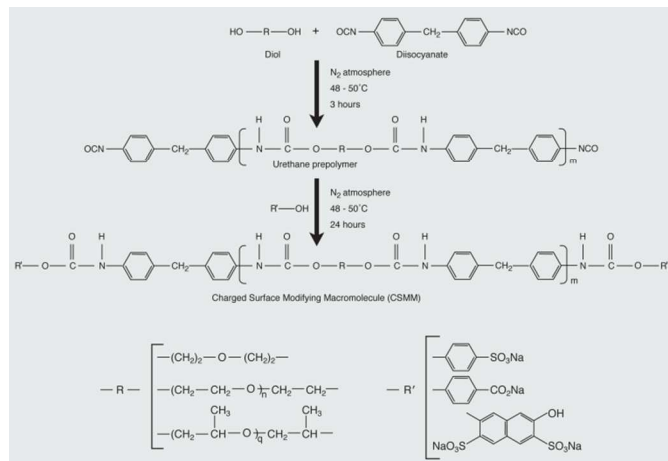


Fig. 1. The schematic presentation of the CSMM synthesis reaction.

A similar process was used for synthesis of the seven CSMMs. In all cases, the molar ratio of the MDI (hard segment): diol (soft-segment): end-capping group was 3:2:2. For example, the PPG-HBC synthesis is as follows. To eliminate the effects of moisture, the glass apparatus was dried at 120°C, and the prepolymerization reaction and end capping steps were performed in a controlled atmosphere of nitrogen inside the reaction vessel. First, 0.1 mole (42.5 g) of degassed PPG was dissolved in 500 mL of degassed DMAc. Second, 0.15 mole (37.5 g) of MDI dissolved in 250 mL of degassed DMAc in a 2L Pyrex round bottom flask with a stirrer. Third, the first solution was added drop wise to the second solution and mixed for 3 h. The temperature was controlled at 48-50°C. Then 0.1 mole (13.22 g) of hydroxyl benzene sulfonate sodium salt, HBS, dissolved in 250 mL of degassed DMAc, was added drop wise. The solution was stirred for 24 h at 48-50°C, resulting in a solution of PPG-HBS. The CSMM solution was added drop wise into a 4L beaker filled with distilled water under vigorous stirring to precipitate the CSMM. The CSMM was filtered in a Büchner funnel and washed with water in order to leach out residual solvent, and dried in an air circulation oven at 120°C for 3 days.

The key features of these tailor-made CSMMs are: a) they contain a backbone that is miscible (compatible in molecular scale) with PES, the principal membrane making polymer used in this study; b) the polyurethane segment of CSMMs insures strong entrenchment in the PES membrane which minimizes leaching; and c) they are charged. Note that in order to produce good membranes these additives have to mix well with the base polymer (PES), otherwise defective membranes will be produced.

Glass transition temperature (T_g)

The glass transition temperature (T_g) was examined by differential scanning calorimeter (DSC) equipped with universal analysis 2000 program (DSC Q1000, TA Instruments, New Castle, DE). Indium was used for the calibration of the temperature. About 10 mg of polymer was crimped into aluminium pan. The polymers were annealed at about $T_g+50^\circ\text{C}$ for 10 min and then quenched to -50°C , and scanned at a heating rate of $10^\circ\text{C}/\text{min}$. The T_g was recorded at the onset and midpoint of the corresponding heat capacity transition.

Membrane preparation

The modified UF membranes were prepared using phase inversion method.²² The casting solutions were prepared by dissolving 18 or 20 wt% PES (as the base or principal polymer) and 3 wt% CSMMs in NMP (i.e., the solvent). First, the CSMM was dissolved in the solvent, then, PES was added and stirred. PES is a popular polymer in the preparation of membranes because it is relatively inexpensive and it is highly resistant to chemicals, such as chlorine.

The details of the casting procedure are as follows: A clean 20.3 x 30.5 cm glass plate was placed on a level surface in a fume hood. A brass casting bar (knife) with a 250 μm gap between the glass and the bar was placed at one end of the plate. The casting solution was poured on the plate next to the casting bar and the casting bar was dragged swiftly over the solution to create a 12.7 x 20.3 cm film with a nominal thickness of 250 μm . For some of these films, a 3 minute rest period was used to allow for enhanced CSMM migration to the surface and enhanced solvent evaporation. This time is called evaporation or drying time. Then the glass plate and film were immersed together into a cold water bath ($4.0\pm 0.2^\circ\text{C}$) for solvent exchange and hardening of the membrane.

Table 2 Characteristic of prepared membranes.

Membrane code	PES (wt%)	CSMM	CSMM (wt%)	NMP (wt%)	Drying time (wt%)
PES18-0	18	-	0	82	0
PES18-3	18	-	0	82	3
PES20-0	20	-	0	80	0
PES18-0/DEG-HBC	18	DEG-HBC	3	79	0
PES18-3/DEG-HBC	18	DEG-HBC	3	79	3
PES20-0/DEG-HBC	20	DEG-HBC	3	77	0
PES18-0/DEG-HBS	18	DEG-HBS	3	79	0
PES18-3/DEG-HBS	18	DEG-HBS	3	79	3
PES20-0/DEG-HBS	20	DEG-HBS	3	77	0
PES18-0/DEG-NDS	18	DEG-NDS	3	79	0
PES18-3/DEG-NDS	18	DEG-NDS	3	79	3
PES18-0/PEG ₂₀₀ -HBS	18	PEG ₂₀₀ -HBS	3	79	0
PES18-3/PEG ₂₀₀ -HBS	18	PEG ₂₀₀ -HBS	3	79	3
PES20-0/PEG ₂₀₀ -HBS	20	PEG ₂₀₀ -HBS	3	77	0
PES18-0/PEG ₄₀₀ -HBS	18	PEG ₄₀₀ -HBS	3	79	0
PES18-3/PEG ₄₀₀ -HBS	18	PEG ₄₀₀ -HBS	3	79	3
PES20-0/PEG ₄₀₀ -HBS	20	PEG ₄₀₀ -HBS	3	77	0
PES18-0/PPG-HBC	18	PPG-HBC	3	79	0
PES18-3/PPG-HBC	18	PPG-HBC	3	79	3
PES20-0/PPG-HBC	20	PPG-HBC	3	77	0
PES18-0/PPG-HBS	18	PPG-HBS	3	79	0
PES18-3/PPG-HBS	18	PPG-HBS	3	79	3
PES20-0/PPG-HBS	20	PPG-HBS	3	77	0

The casting was conducted under three conditions: a) 18 wt% PES casting solution with no evaporation time (PES18-0); b)

Paper

18 wt% PES casting solution with 3 min evaporation time (PES18-3); and c) 20 wt% PES casting solution with no evaporation time (PES20-0). The membranes were called by the code name PES x - y /S-E, where "PES" stands for poly(ether sulfone), " x " is the weight percent base polymer in the casting solution, " y " the evaporation time, and S-E is the CSMM, where S represents the soft segment and E represents the end-cap. The experiment called for the preparation of twenty three membranes using seven CSMMs. The code name and composition of the cast membranes are shown in Table 2.

The PES concentrations were chosen based on prior experiences of the research group.²³ The 18 wt% PES solution produces membranes with suitable performance and increasing the PES concentration leads to tighter membranes. Furthermore, preliminary experiments indicated that membranes made of 21 wt% or higher PES concentrations are extremely tight and offer very low fluxes. Also earlier work with other hydrophobic and hydrophilic SMM additives showed that the incorporation of migration time also leads to tighter membranes, i.e. smaller pores, which should be beneficial in the separation of PPCPs. The 3 min time period was selected based on preliminary experiments using control membranes (PES without CSMMs) and membranes prepared with one of the additives.

Membrane cells and membrane separation system

The flat sheet membranes developed in this study were evaluated in a membrane performance system incorporating six cross flow membrane cells arranged in parallel (Fig. 2). The details of the design of the cell, schematically and photographically, are presented in the supplementary information (Fig. S1).²⁴⁻²⁶ The feed enters through a 1/4" tubing on the side of the cell, it goes towards the centre of the cell and then up to the membrane chamber on top. The membrane is essentially the roof of this chamber, it is placed on a porous stainless steel grit support and is sealed using a rubber O-ring. The permeate passes through the membrane and exits through a 1/8" tubing at the side of the upper part of the cell. The retentate travels radially along the surface of the membrane and exits the membrane chamber through a 0.6 mm collection gap (h_{gap}) at the outer edge of the top portion of the cell and down to the 1/4" tubing shown as "Retentate" in the Fig. S1. The cross flow membrane cells have an effective membrane area of 20.4 cm². Two sets of independent six-cell membrane performance systems were built. Each system consisted of a large feed tank, six membrane cells, pressure gauges, valves, and a retentate cooling system. In each system the feed was pumped from its feed tank by its pump. A flow meter located before the first feed distribution point measured the overall flow of the feed. The feed flow rate to each separation cell was controlled by two metering valves installed at the feed and the retentate sides of the cell. The permeate was collected individually from each cell and returned to the feed tank. A pressure gauge located before distribution of the feed was used to measure the total feed pressure. Six individual pressure gauges were installed at the feed side of the membrane cells to measure the individual feed pressure. A 3-way valve was installed at the retentate side of each cell to be able to redirect the retentate through a downstream flow-meter (prior to returning it to the feed tank) to help balance the flow equally among the six cells. Most of the time, the 3-way valves directed the retentate to the heat exchanger (connected to a recirculating cooling bath) before returning to the feed tank. The heat exchanger was installed to prevent a water temperature rise.

Prior to the experiments the membrane cells were cleaned using an ultrasonic bath to ensure removal of any contamination remaining from previous experiments. The cells were then tested by analysing the total organic carbon (TOC) concentration of the circulating water before and after cleaning using a low-level UV-persulfate oxidation based TOC analyser (Phoenix 9000, Teledyne-Tekmar, Mason, OH). The cleaning procedure was repeated until no contamination was found in the water.

Membrane characterization

Membrane characterization was conducted via contact angle, Fourier transform infrared (FTIR) spectroscopy, surface charge, pure water permeation, and solute transport measurements.

Contact angle (CA) measurement

Static contact angle (CA) measurements were conducted using a goniometer that incorporates a digital camera (VCA Optima Contact Angle Analyser, AST Products Inc., Billerica, MA). The instrument uses a mechanically driven syringe to add 0.5 μ l of water to a water droplet placed on the surface of the membrane; the membrane sample was taped to a glass slide to facilitate the imaging. The droplet was constantly monitored by the camera. At some point the pressure in the droplet causes it to slip and expand. The camera retains the image of the droplet immediately before the movement and the system calculates the static CA based on this image of the water/glass/air interface. Because the static CA varies somewhat over the surface of the membrane, for each membrane type at least three membrane samples were used and three measurements were taken from each sample. The average value is reported.

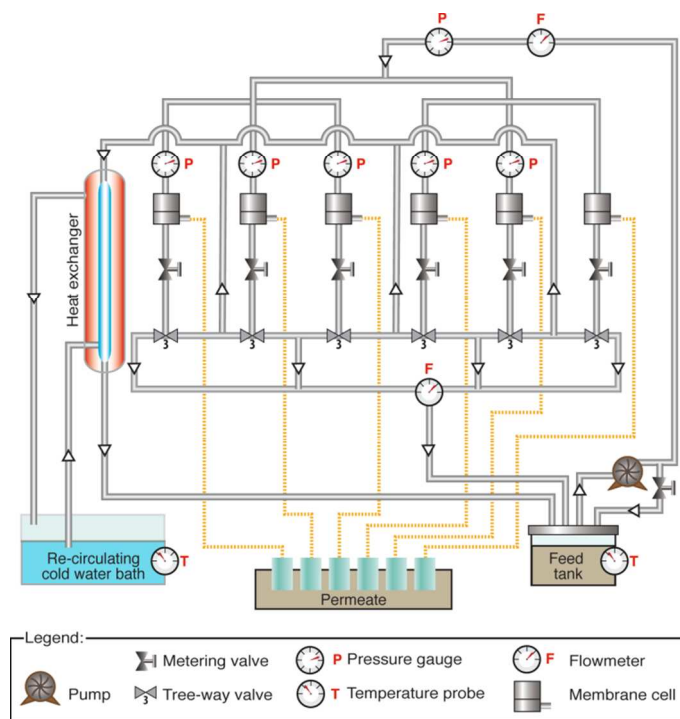


Fig. 2. Schematic of the membrane filtration set up.

Fourier transform infrared (FTIR) measurement

Fourier transform infrared (FTIR) spectroscopy was used to observe the presence of functional groups of the membrane. The FTIR spectrometer (Varian 1000, Scimitar series, Varian Inc., Palo Alto, CA) was equipped with diamond w/ZnSe lens single reflection attenuated total reflection (ATR) plate. An IR source at 45° incident angle was employed. The membranes, in dry as well as wet state, were mounted on the crystal surface to examine the structure of either top or bottom layer of the membrane. The spectra were measured in transmittance mode over a wave number range of 4000 to 600 cm⁻¹ at a resolution of 4 cm⁻¹.

Surface charge (SC) measurement

Zeta potential, an indicator of the membrane surface charge, was determined using a modified system based on the description provided by Szymczyk et al.²⁷ Ag/AgCl electrodes were prepared with anodic deposition of chloride on silver from a 0.001 M HCl solution with a current density of about 0.2 mA/cm². The electrodes were stored in 0.5 M KCl solution overnight to prevent build-up of charge. All the measurements were performed at room temperature (25±0.5°C), pH 7±0.1 and 0.001 M KCl solution as the electrolyte. Zeta potentials were calculated from the relation of streaming potential versus differential pressure using the Helmholtz-Smoluchowski equation.²⁸ The background electrolyte for streaming potential determination was potassium chloride (KCl). Potassium hydroxide (KOH) and hydrochloric acid (HCl) were employed to adjust the pH. In order to measure streaming potential, a membrane coupon (20 cm²) was inserted into the membrane cell. A 0.001 M solution of potassium chloride (KCl) was sequentially filtered at five increasing pressures ranging from 1 to 30 kPa (10 to 300 mbar) through the cell. Temperature and pH were monitored on the feed side of the membrane and adjusted using ice and hot water baths, and hydrochloric acid (0.1M HCl) and potassium hydroxide (0.1M KOH) solutions, respectively. The difference in current (streaming potential) between the silver chloride electrodes, placed on the feed and permeate sides of the membrane, was measured. By measuring the streaming potential at different pressures, a plot of streaming potential versus pressure was generated. Using linear regression, the slope of the best line of fit was used to calculate the variation in streaming potential with pressure. The zeta potential can then be determined using the Helmholtz-Smoluchowski equation (1)²⁸:

$$\zeta = \frac{\Delta E}{\Delta P} * \frac{\eta \kappa}{\epsilon_o \epsilon_r} \quad (1)$$

Where ΔE is the variation in streaming potential (mV), ΔP is the variation in transmembrane pressure (mbar), η is the permeate viscosity, κ is the solution conductivity, ϵ_o is the vacuum permittivity and ϵ_r is the dielectric constant of the media. The experimental set-up of the streaming potential measurement is shown in the supplementary information (Fig. S2). For details of this method refer to previous publications.^{29, 30}

Membrane filtration

The membrane performance tests consisted of two parts: a) pure water permeation (PWP) test; and b) solute testing to determine the molecular weight cut-off (MWCO), pore density (N) and surface porosity (S_p).

Pure water permeation (PWP) test

The pure water permeation tests were conducted using the two six-cells-in-parallel systems using Milli-Q water as the feed. The testing protocol consisted of a 1 h pre-compaction step at 80 psig, followed by a 50 h filtration cycle with a transmembrane pressure of 50 psig. The feed flow rate was 0.65 L per cell. The 50 h duration of the pure water test is based on previous experience regarding flux stabilization for PES membranes.²³

The pure water permeation flux can be reported in a number of different ways including the normalized standard flux (NSF) which is defined using equation (2):

$$NSF = J_{SP}^{22} = J_{SP}^T \cdot \frac{\mu (@ T^{\circ}C)}{\mu (@ 22^{\circ}C)} = \frac{Q_p^T}{A_{mem} \cdot \Delta P} \cdot \frac{\mu (@ T^{\circ}C)}{\mu (@ 22^{\circ}C)} \quad (2)$$

Where NSF = J_{SP}^{22} is normalized standard flux at 22°C (L/m² h bar); J_{SP}^T is normalized standard flux at temperature T°C (L/m² h bar); Q_p^T is permeate flow rate at temperature T (L/h), A_{mem} is membrane area (m²), ΔP is transmembrane pressure (bar); μ is water viscosity (N s/m²).

Solute transport tests

The solute transport tests involved the filtration of at least five different solutions prepared with PEO of 100 kDa and/or PEG solutions with different molecular weights (0.4, 0.6, 1, 1.5, 4, 6, 8, 14, and/or 35 kDa). The feed solute concentrations were approximately 200 mg C/L, measured using a thermal-oxidation-based TOC analyser (Phoenix 9000, Teledyne-Tekmar, Mason, OH). The testing period for each solution was 1 h which was followed by filtration of Milli-Q water for at least 1 h before the feed was changed to the next test solute. The operating pressure was 50 psig and the flow rate per cell was 0.65 L/min. Based on the removal of these solutes the pore size distribution and MWCO were determined. The removal data for these solutes were plotted versus solute molecular weights, and the MWCO corresponded to 90% removal. MWCO is a characterization parameter that is routinely reported by membrane manufacturers.

The following is from the development by Singh et al.³¹ The pore size distribution of a given UF membrane can be characterized by log-normal distribution shown in equation (3):

Paper

Journal of Materials Chemistry A

$$\frac{df(d_p)}{dd_p} = \frac{1}{d_p \ln \sigma_p \sqrt{2\pi}} \exp \left[-\frac{1}{2} \left(\frac{\ln(d_p / \mu_p)}{\ln \sigma_p} \right)^2 \right] \quad (3)$$

Where d_p is the pore diameter, μ_p is the geometric mean of the pore diameter and, σ_p is the geometric standard deviation of the pore diameter. The μ_p is determined from the 50% probability of solute diameter ($f = 50\%$) and the σ_p can be calculated as follows in equation (4):

$$\sigma_p = \frac{\text{solute diameter at } f = 84.13\%}{\text{solute diameter at } f = 50\%} \quad (4)$$

It is assumed the solute diameter is equivalent to the pore diameter and that their geometric standard deviations are the same.

The particle size of the probe solutes, PEG and PEO, is estimated using the respective Stokes radius (a) expressions, which are function of the molecular weight (MW) of the probe solutes. Stokes radius is used since it approximates the radius based on the assumption that the particle behaves as a hypothetical sphere which diffuses similarly to the particle (probe solute) in question.

$$\begin{aligned} a_{PEG} &= 16.74 \times 10^{-10} MW^{0.557} \\ a_{PEO} &= 10.44 \times 10^{-10} MW^{0.587} \end{aligned} \quad (5)$$

The above expressions (5) are based on empirical expressions of intrinsic viscosities and the Stokes-Einstein diffusivity expressions, as derived by Singh et al.³¹

The Hagen-Poiseuille equation, modified for porous membranes and assuming laminar flow, is the basis for the expressions for the pore density (N) as demonstrated in equation (6).

$$N = \frac{128\eta\delta J}{\pi\Delta P \sum_{d_{\min}}^{d_{\max}} f_i d_i^4} \quad (6)$$

Where η is the solvent viscosity (N s/m²), δ is the pore length (the thickness of the dense skin layer of the asymmetric membrane based on the assumption of no pore tortuosity) (m), ΔP is the transmembrane pressure (Pa) and J is the membrane flux (m³/m²/s).

From this, the surface porosity (S_p) can be determined as shown in equation (7):

$$S_p = \left(\frac{N\pi}{4} \sum_{d_{\min}}^{d_{\max}} f_i d_i^2 \right) * 100\% \quad (7)$$

Using the removal performance of the test membranes for various sizes of probe solutes, the MWCO could be estimated. Likewise, the surface porosity could be quantified by using the flux and transmembrane pressure at the corresponding operating conditions. Finally, the pore size distribution can be determined from the log-normal probability as a function of the solute removals. To determine the MWCO, the probability of removal is plotted against the logarithm of the Stokes radius of the various probe solutes tested. From this data, a linear regression is traced. The MWCO is determined based on the probability of 90% removal from the linear regression. The geometric standard deviation is determined from the 84.13% probability of the same regression as well as the 50% removal, which gives the mean pore size. MWCO, geometric standard deviation, mean pore size, pore density, and porosity were determined for each of the three coupons (of each type of membrane) and the average of those values are reported.

Experimental protocol of EDC and PPCPs removal

The protocol involved a screening process where the removal efficiencies of all cast membranes were determined using sequential testing with solutions of Milli-Q water spiked with single PPCPs. It is noted that the pH of the test solutions was not adjusted. These filtration tests were conducted immediately after the standard solute (PEG, PEO) tests using the same membrane coupons used in the PWP tests and the solute transport tests. In this procedure one solute was tested at a time, and rinsing cycles were conducted between each test. The primary reason for testing one PPCP at a time at a relatively high concentration (ppm levels) was to permit chemical analysis using a TOC analyser rather than sophisticated and expensive analytical methods available for extremely low concentrations of PPCPs. The disadvantage of TOC analysis was the limited sensitivity of UV-persulfate based TOC analyser that required PPCP concentrations in the order of 10 mg C/L. Such concentration is much higher than the environmental occurrence of these substances. Despite this drawback, the use of the TOC analyser greatly simplified the logistics of the membrane screening process. During this testing the membrane filtration system was operated at 50 psi and a flow rate per cell of 0.65 L/min.

It was expected that at high PPCP concentrations, a portion of the PPCP would adsorb on all surfaces of the system. For this reason, a thorough rinsing procedure was developed and tested to ensure no contamination remained in the system from previous experiments. The four PPCPs and EDC were selected to have a range of different MWs and different degree of hydrophilicity, Log octanol-water partition coefficient (Log K_{OW}). The selected compounds were: BPA, CARB, IB, and SMZ. Three of these compounds are PPCPs (CARB, IB, SMZ), and one is an EDC (BPA). IB presented its own challenges as the TOC measurements were significantly lower than expected. This seems plausible given the much higher values of the Henry's law constant and vapour

pressure of ibuprofen compared to that of the other EDC and PPCPs tested.³² The problem appeared to be caused by volatilization during the CO₂ stripping step of the analysis. This problem was solved by using total carbon measurements instead of TOC. The results indicated that BPA, CARB, IB and SMZ were dissolved to a level of at least 20 mg C/L within 24 h (except IB which took up to 48 h) at ambient temperature.

Prior to each of the one hour filtration runs with one of the target compound solutions, the filtration system was cleaned for 30 min with Milli-Q water. For 20 min the system was operated on a flow-through basis and in the next 10 min the system was operated in a recycle mode. The two six-cells-in parallel systems were operated simultaneously. Their flow rate was 0.65 L/min per cell. As the systems were operated on a flow through basis during the rinsing cycles, the Milli-Q water demand was approximately 250L per day.

The baseline TOC content of the Milli-Q water in this study was in the range of 0.05 to 0.1 mg C/L. The precision of the TOC measurement was $\pm 2\%$ or better. Separate calibration curves were developed for each compound. Also, a potassium biphthalate standard curve was found to describe all compounds well.

3. Results and discussion

Glass transition temperature (T_g)

The glass transition temperature of polymer indicates a transition point between amorphous and rubbery state. From Table 3, it can be seen that PPG-HBS has the lowest T_g indicating it is the most flexible while DEG-NDS has the highest indicating it is the most rigid probably due to the very rigid NDS end groups. It is further noted that the onset and midpoint T_g of PES are 221.4°C and 225.4°C, respectively.

Table 3 Glass transition temperatures of CSMMs.

CSMMs	T_g (°C) at onset	T_g (°C) at midpoint
DEG-HBC	114.5	131.6
DEG-HBS	94.8	101.3
DEG-NDS	> 300	> 300
PEG ₂₀₀ -HBS	62	68.5
PEG ₄₀₀ -HBS	6.8	13.4
PPG-HBC	106	111.3
PPG-HBS	-18.3	-11.6

Characterization of membranes

The properties and performance of the twenty three PES membranes prepared in this study were characterized and then tested in the removal of one EDC and three PPCPs.

Static contact angles (CAs)

The addition of the CSMMs and their migration to the membrane surface was expected to impart a negative charge upon the membranes, which in turn would result in more hydrophilic

membranes with smaller CAs. Fig. 3 presents the static contact angle results of all the prepared membranes. It shows that in most cases the contact angles remained statistically the same as the control membranes or increased slightly (more hydrophobic). It is to be noted that contact angle is not a micro-property controlled by the surface charge alone, but more of a macro-property which is also affected by the roughness of the membrane surface.³³ Thus, it appears that the CSMMs did not significantly change the contact angle of the PES membranes because: a) the CSMMs also caused a change in the surface roughness; and/or b) the CSMMs did not significantly migrate to the surface; and/or c) the charge they imparted was too small.

However other membrane characterization described seems to indicate that there was migration.^{34, 35} The migration of CSMM to the membrane surface was confirmed with respect to hollow-fiber nanofiltration membranes containing PEG₂₀₀-HBS in PES by X-ray photoelectron spectroscopy. Both sulfur and oxygen concentration increased at the outer surface of the hollow-fiber membranes due to the PEG₂₀₀-HBS migration.³⁴ It is noted that both CSMMs blended and control PES UF membranes exhibited a nodular structure and the size of nodular aggregates measured by atomic force microscopy ranged from 25 to 75 nm. The size of nodular aggregates decreased by blending PEG₂₀₀-HBS in PES membrane.³⁵

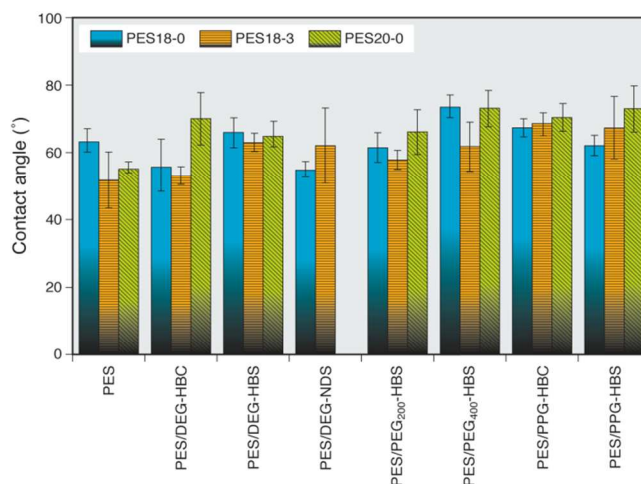


Fig. 3. Static contact angle of modified and control membranes as a function of CSMMs and casting condition.

Fourier transform infrared (FTIR)

The presence of functional groups at the surface of the asymmetric membranes was examined by FTIR-ATR spectroscopy. The FTIR spectra taken from the bottom and the top surface of the control PES membrane as well as PES/DEG-HBS membrane in their dry form are shown in Fig. 4a. It is highly noted that spectra of the top and bottom surfaces are almost identical for both membranes. The spectrum of the PES membrane shows the peaks at 1578 and 1486 cm⁻¹, which are for aromatic bands. The sharp adsorption peaks at 1323 and 1150 cm⁻¹ are assigned to the asymmetric and symmetric stretching vibration of sulfone (O=S=O) group, respectively. The sharp adsorption peak at 1239 cm⁻¹ is due to stretching vibration of aromatic ether (Ar—O—Ar) linkage. On the other hand, peaks

Paper

corresponding to DEG-HBS additive appeared in the spectrum of the PES/DEG-HBS membrane on top the peaks corresponding to PES. The additional peaks of DEG-HBS are: 1728 and 1527 cm^{-1} which can be assigned to aliphatic ether peak ($\text{CH}_2\text{—O—CH}_2$) of DEG segments and amide (CO—NH) group. Then the FTIR subtraction spectra (wet surface minus dry surface) are shown in Fig. 4c for each membrane surface. As expected, the presence of water is visualized for all membrane surfaces as a broad peak at 3370 cm^{-1} . The sharp peak at 1640 cm^{-1} for the PES membrane, both at the top and the bottom surface, is due to the interaction of aromatic ether group of PES with water as O—HO bonds. The broad peaks at 1709 and 1640 cm^{-1} for PES/DEG-HBS membrane, both at the top and the bottom surfaces, are due to the interaction of aliphatic ether group of DEG-HBS with water as O—HO bonds and also aromatic ether group with water as O—HO bonds. The sharp peaks at 1125, 1250 and 1300 cm^{-1} are due to the interaction of sulfonate (SO_3^-) group of DEG-HBS with water as S—O—HO bonds. In the literature, interaction of sulfonate with water peaks has appeared in the ranges of 1100–1200 and 1300–1420 cm^{-1} . These results confirm the presence of DEG-HBS in the membrane when DEG-HBS was blended in PES and also the interaction of water with the functional groups present in the membrane.

With great importance it is highly noted that the state of water in the CSMMs incorporated membrane was determined by our earlier DSC study, showing that the amount of the bound water increased by CSMM (in particular PEG₂₀₀-HBS) incorporation in PES base polymer.³⁶ It is also noted that T_g of the PES/PEG₂₀₀-HBS blended membrane yields a single T_g, indicating a miscible blend system, and a positive deviation in the Gordon–Taylor equation, which means the presence of strong segmental interaction between PES and PEG₂₀₀-HBS. In fact strong specific interactions, such as charge transfer, hydrogen bonding, etc., may exist between PES/PEG₂₀₀-HBS segments. The PEG₂₀₀-HBS contains both ends sulfonate group which could strongly interact with the sulfonyl group of PES.³⁶

Surface charge (SC)

The blending of CSMMs was expected to give the PES membranes a more negative surface charge, but Fig. 5 shows that no statistically significant trend could be concluded. The most striking characteristics of the charge measurements are that the magnitude of the measured zeta potential was rather small compared to the -13 mV to -90 mV range reported for commercial PES membranes.^{37–39} Surprisingly, significant differences were observed among the control PES membranes (without the addition of CSMM) when manufactured under different conditions. In addition, some additives, like DEG-HBC, DEG-NDS and PPG-HBC, caused the surface charge to increase under certain membrane preparation conditions, while caused it to decrease under other conditions. For the three different manufacturing conditions the membranes prepared with DEG-HBS and PPG-HBC had higher average surface charge than the controls. It should be noted that there is a significant variability in the measurements. This seems to indicate that CSMMs do not impart a significant charge on the PES membranes. It should be noted that all the CSMM blended PES₂₀₋₀ membranes showed more negative surface charges than the control PES₂₀₋₀ membrane, while they showed higher CAs than the control PES₂₀₋₀ membrane. This strongly suggests that the contact angle measurements are significantly affected by factors other than surface charge.

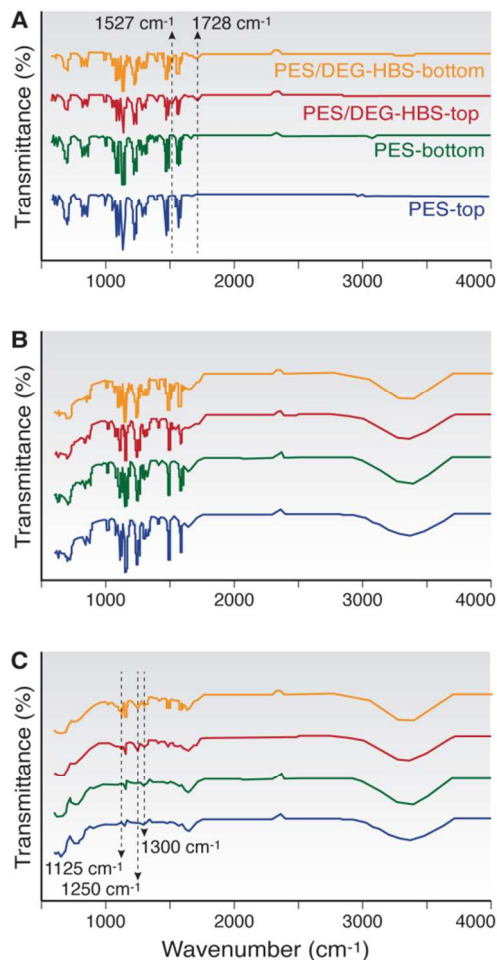


Fig. 4. Representative FTIR spectra of top and bottom surfaces of PES and DEG-HBS blended PES membranes dry membranes: (A) dry membrane surface, (B) wet membrane surface, and (C) subtraction (dry-wet) spectra.

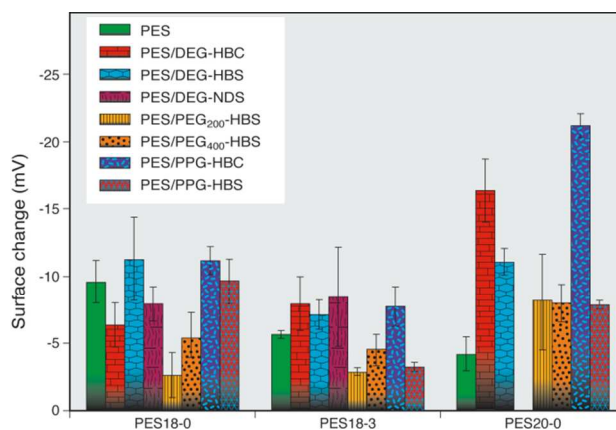


Fig. 5. Surface charge of modified and control membranes as a function of CSMMs and casting condition.

Membrane permeation performance

The NSF of the membranes tested are presented in Fig. 6. Comparing the control membranes it is evident that an increase in solvent evaporation time from zero to 3 min and an increase in PES concentration from 18 to 20 wt% both decreased the flux. This trend was expected as increasing evaporation time or increasing the base polymer concentration generally results in tighter membranes.^{23, 40} For the membranes incorporating CSMMs, the patterns were irregular; the membranes with PPG-HBC showed the same pattern as the control membranes while the opposite pattern was observed for the PPG-HBS membranes. From these results, it could be concluded that each CSMM behaves differently. These NSF values are significantly smaller than the 30-58 L/m² h bar reported for commercial UF membranes.⁴¹

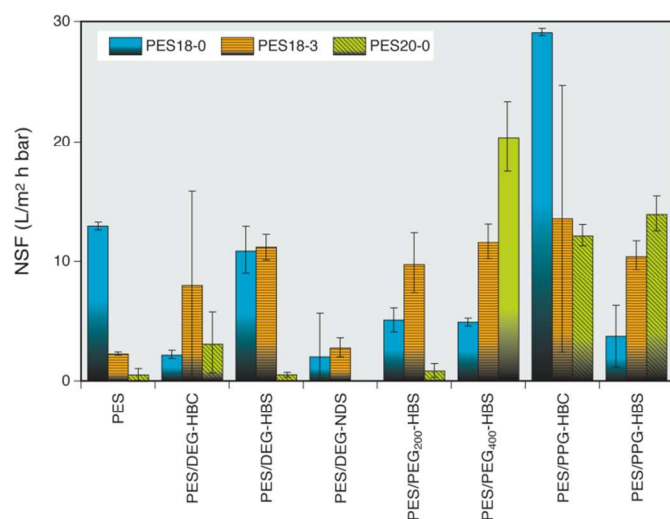


Fig. 6. Normalized standard flux (NSF) of modified and control membranes as a function of CSMMs and casting condition.

Table 4 Characteristic of filtration performance data of membranes.

Membrane code	NSF (L/m ² h bar)	MWCO (kD)	Pore size (nm)	Pore density (pores/μm ²)	Porosity (%)
PES18-0	13.0±0.2	62.5±6.7	4.2±0.0	4942±327	7.1±0.4
PES18-3	2.2±0.1	34.0±3.0	1.3±0.2	743±133	1.2± 0.1
PES20-0	0.4±0.5	41.6±8.3	1.4±0.7	198±175	0.3± 0.1
PES18-0/DEG-HBC	2.1±0.3	9.8±1.4	1.2±0.0	466±427	0.8±0.3
PES18-3/DEG-HBC	7.8±8.3	9.1±0.5	1.1±0.0	2865±3326	4.1±4.3
PES20-0/DEG-HBC	3.1±2.6	27.0±27.3	1.4±0.5	409±227	1.1±0.8
PES18-0/DEG-HBS	10.9±1.9	31.6±3.6	1.5±0.1	3907±1192	5.9±1.1
PES18-3/DEG-HBS	11.2±1.1	24.4±1.1	2.3±0.1	3805±993	5.7±0.4
PES20-0/DEG-HBS	0.4±0.2	12.9±3.5	1.0±0.0	169±95	0.2±0.1
PES18-0/DEG-NDS	2.0±3.5	10.8	1.0	754±1297	1.2±2.0
PES18-3/DEG-NDS	2.7±0.7	35.5±11.7	1.5±0.1	538±398	1.0±0.3
PES18-0/PEG200-HBS	5.0±0.9	32.6±13.8	2.3±0.0	498±26	0.0±0.0
PES18-3/PEG200-HBS	9.8±2.5	49.4±19.9	2.2±0.3	3228±1416	4.7±1.2
PES20-0/PEG200-HBS	0.8±0.5	93.8±53.0	2.0±0.0	295±192	0.4±0.3
PES18-0/PEG400-HBS	4.8±0.3	28.7±2.6	1.3±0.1	1200±1009	1.9±0.6
PES18-3/PEG400-HBS	11.6±1.4	55.7±8.0	2.2±0.0	3011±2636	4.7±1.9
PES20-0/PEG400-HBS	20.5±2.9	26.5±23.2	1.4±0.8	2036±557	6.3±1.2
PES18-0/PPG-HBC	29.0±0.2	69.8±37.3	3.0±1.0	7030±6183	11.4±3.6
PES18-3/PPG-HBC	13.6±11.2	83.0±43.3	1.9±0.4	2855±2762	5.2±4.0
PES20-0/PPG-HBC	12.2±0.9	52.7±4.1	3.2±0.4	1190±75	3.7±0.1
PES18-0/PPG-HBS	3.7±2.6	44.2±19.4	1.0±0.0	1345±1098	1.9±1.3
PES18-3/PPG-HBS	10.4±1.2	80.0±11.4	2.6±0.3	3320±263	5.0±0.6
PES20-0/PPG-HBS	14.0±1.4	40.7±6.5	2.7±0.5	1368±44	4.3±0.2

Solute separation tests were conducted to estimate the membrane pore size, porosity, pore density and MWCO.^{31, 42} The characteristics of the membrane filtration performance including membrane pore size, porosity, pore density, MWCO and NSF is presented in Table 4. In earlier work with SMMs, an increase in the polymer concentration and an increase in solvent evaporation time resulted in lower fluxes and smaller pore sizes.⁴² This was the case for the control membranes (Fig. 7) since MWCO has become smaller. And for the PES18-0 membranes the blending of six out of the seven additives resulted in significantly lower MWCO, however generally this was not the case for the PES18-3 and PES20-0 membranes. The decrease in the MWCO of the modified PES18 membranes may be more apparent because the control PES18-0 membrane had a higher MWCO than the other control membranes. Among the membranes incorporating CSMMs, the same pattern was observed only for DEG-HBS, while the patterns were different for the other CSMMs. The most important results shown in these figures are: a) the majority of the MWCOs are in the 20 to 50 kDa range; and b) the lowest MWCOs are approximately 10 kDa.

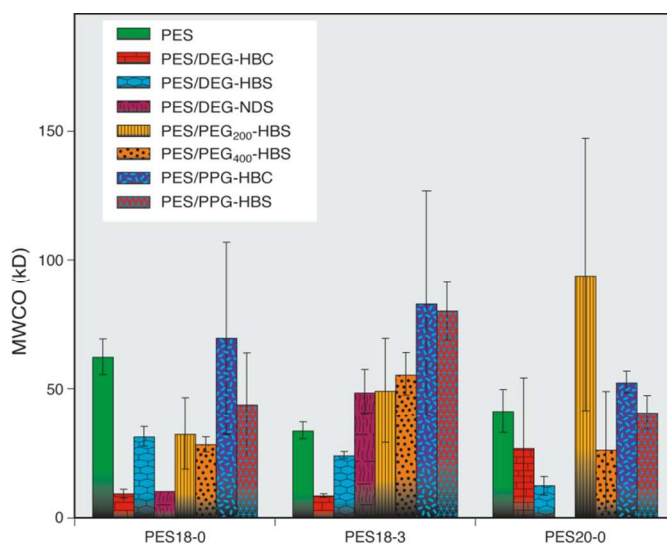


Fig. 7. Molecular weight cut-off (MWCO) of modified and control membranes as a function of CSMMs and casting condition.

The relationship between NSF versus surface charge is shown in Fig. 8. This figure shows an overall pattern of increasing NSF with increasing negative surface charge, which is expected. The line shows the pattern for the control PES membranes, and many of the modified membranes achieved higher fluxes for the same surface charge.

When membranes are operated at a given pressure, there is a general relationship of increasing NSF with increasing pore size and MWCO; i.e. the flux increases because often the number of pores does change significantly so increasing the pore size increases the membrane porosity. In trying to develop better membranes, the objective is to produce membranes that show positive deviations from this relationship, i.e. higher fluxes than those predicted by the general relationship for the MWCO in question. The dashed line in Fig. 9 indicates that the NSF-MWCO relationship for the control PES membranes follows this pattern and several of the CSMM

Paper

modified membranes resulted in positive deviations from the general trend. All of the PES/DEG-HBC, PES/DEG-HBS and PES/PEG₄₀₀-HBS membranes had positive deviations from the pattern of the control PES membranes. The PES18-3/PPG-HBC (MWCO ~69.8 kDa) and PES20-0/PEG₄₀₀-HBS (MWCO ~28.7 kDa) (circled in Fig. 8) had an excellent compromise between NSF and MWCO. DEG-HBC and DEG-NDS produced some of the tightest membranes (MWCO ~9 to 11 kDa), and the PES18-3/DEG-HBC membrane appeared to be the most promising because of its low MWCO, and it has the highest flux among the tightest membranes. With sufficiently high flux and relatively small MWCO, these membranes seem promising, but the true test is the membrane's ability to separate EDC and PPCPs.

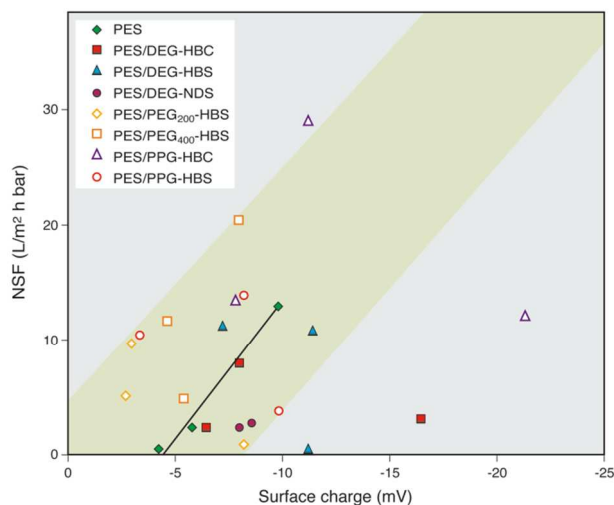


Fig. 8. NSF versus membrane surface charge for control and CSMMs blended membranes.

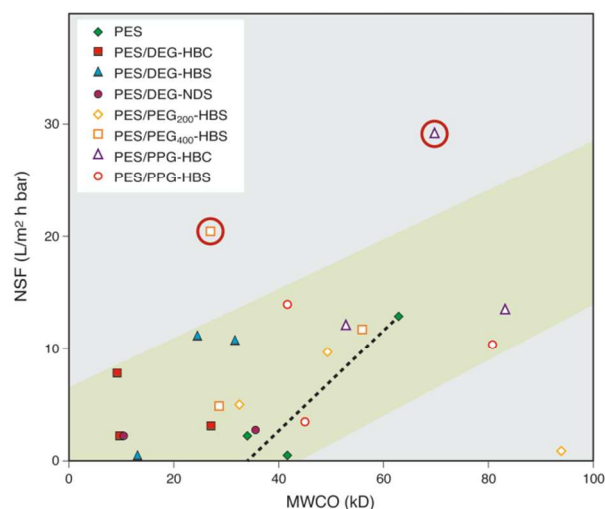


Fig. 9. NSF versus MWCO for control and CSMMs blended membranes.

The plot of correlation between NSF versus surface porosity which is defined as the ratio between the areas of pores to the total membrane surface area (eq. (7)) is shown in Fig. 10a. As discussed above, the PES18-0/PPG-HBC and PES20-0/PEG₄₀₀-HBS membranes show higher fluxes and this is attributed to their higher porosity. Regardless of the CSMM blended in the membrane, there is a direct correlation between NSF and porosity, which is expected since they are linked (NSF is involved in the estimation of surface porosity). The higher NSF values of the better membranes identified above (i.e., PES18-0/PPG-HBC and PES20-0/PEG₄₀₀-HBS) resulted from having a higher porosity. Fig. 10b shows that the increase in NSF is related to pore density and that different CSMM appear to result in fairly consistent pore densities.

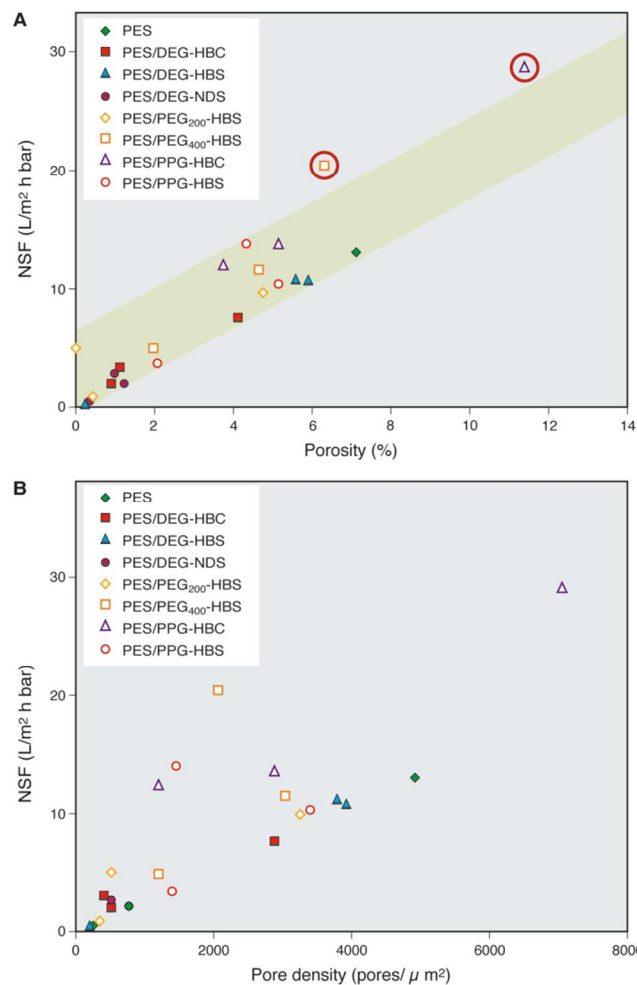


Fig. 10. (A) NSF versus porosity and (B) NSF versus pore density for control and CSMMs blended membranes.

Membrane removal performance of EDC and PPCPs

The BPA, CARB, IB, and SMZ removal data for the single solute tests for all the membranes is presented in Table 5. As discussed, PES18-3/PPG-HBC and PES20-0/PEG₄₀₀-HBS have higher NSF performance but the EDC/PPCPs removal efficiency of these two membranes is inferior to that of some of the other

Journal of Materials Chemistry A

Paper

membranes. It is noted that the 20 wt% PES with PES20-0/PEG₂₀₀-HBS membrane had much higher percent EDC and PPCP removals than the other membranes. Moreover, only the PES18-0/PPG-HBS membrane shows CARB removals similar to that of the PES20-0/PEG₂₀₀-HBS membrane (20.6% versus 22.1% removal). Both these membranes have average fluxes.

Table 5 Characteristic of filtration performance data of membranes.

Membrane code	BPA (%)	CARB (%)	IB (%)	SMZ (%)
PES18-0	6.67±3.91	0	12.66±3.49	0.88±1.06
PES18-3	28.25±35.80	11.58±0.56	21.78±4.94	9.52±0.37
PES20-0	17.32±12.13	0	22.65±1.45	2.85±4.21
PES18-0/DEG-HBC	21.44±10.29	9.85±1.02	17.26±3.10	5.29±0.98
PES18-3/DEG-HBC	12.62±14.60	5.72±6.31	5.42±0.10	3.02±1.63
PES20-0/DEG-HBC	20.78±18.41	5.97±4.21	7.50±0.31	4.35±1.74
PES18-0/DEG-HBS	0	0.36±0.08	3.67±2.09	0.95±0.63
PES18-3/DEG-HBS	0	0	0	1.88±0.06
PES20-0/DEG-HBS	30.84±31.19	8.49±9.30	21.35±9.13	8.39±13.26
PES18-0/DEG-NDS	6.01	0.84	12.57	5.39
PES18-3/DEG-NDS	30.35±9.77	13.20±3.69	24.60±3.77	7.04±3.51
PES18-0/PEG ₂₀₀ -HBS	19.84±21.85	5.82±9.72	24.38±24.38	7.03±6.85
PES18-3/PEG ₂₀₀ -HBS	15.57±18.72	3.07±5.25	9.33±5.14	1.91±2.24
PES20-0/PEG ₂₀₀ -HBS	53.05±7.58	22.09±2.03	54.20±4.84	20.90±8.11
PES18-0/PEG ₄₀₀ -HBS	7.47	0	6.70	5.48
PES18-3/PEG ₄₀₀ -HBS	0.09±0.08	0	0.05±0.00	0.01±0.00
PES20-0/PEG ₄₀₀ -HBS	6.35±1.25	0	6.56±1.00	0
PES18-0/PPG-HBC	0	0	0	0.70±1.73
PES18-3/PPG-HBC	17.99±2.00	0	7.20±2.23	0
PES20-0/PPG-HBC	1.44±1.12	0	6.13±1.95	0
PES18-0/PPG-HBS	26.06±14.69	20.65±10.78	27.82±14.68	4.85±4.35
PES18-3/PPG-HBS	18.31±0.96	0	6.54±2.01	0.11±0.40
PES20-0/PPG-HBS	0.67±0.46	0.44±0.74	2.27±0.71	1.49±0.42

The order in the Log K_{OW} is SMZ < CARB < BPA < IB. Considering that the larger Log K_{OW} means the lower partition of solute to the aqueous phase, the above order indicates that IB is the most likely to be strongly adsorbed to the membrane, while SMZ is the least likely. The highest percent SMZ, CARB, BPA and IB percent removals observed were 20.9, 22.1, 53 and 54.2, respectively. This suggests that the adsorption effect governs the EDC/PPCPs separation. It is well established that micro-pollutants adsorb to membrane surfaces.⁴³ The main interaction forces are due to hydrophobic and solvation effects. The interplay of molecular and supra-molecular interactions such as hydrogen bonding, π - π stacking, ion-dipole, and dipole-dipole interactions also contributed. Many functional groups and aromatic rings involved both in PES and the EDC/PPCPs molecules enable such attractive interaction. Hence, the force working between the membrane surface and the EDC/PPCPs is also an important criterion to determine the EDC/PPCPs micro-pollutant adsorption. Although the importance of charge repulsion is expected to be pH dependent, the pH of the test solutions was not adjusted as this is not expected to be a part of full-scale treatment.

It is noted that the order in molecular weight is SMZ > CARB > BPA > IB. Therefore, the sieving effect does not appear to play a role in the EDC/PPCPs separation. This is not surprising given that the target compounds had molecular weights in the 200 to 300 Dalton range while the MWCO of the membranes were >10 kDa. Hence size exclusion is not expected to play a significant role in the separation of the target compounds by these membranes.

The above removal information was for short term tests. To confirm the role of adsorption a number of longer tests were conducted with two membranes (PES18-0/PEG₂₀₀-HBS and PES18-

3/PEG₂₀₀-HBS). Their results are shown in Fig. 11a and 11b, respectively. In all the cases the general pattern of the membrane performance was the same. Initially the EDC and PPCPs removal was high, up to 55%, but gradually declined to zero or would have declined to zero if the runs were continued (Fig. 11). This pattern indicates that charge repulsion and size exclusion, the principal mechanisms expected to control EDC and PPCPs removal, were not significant and that initial removal was the result of adsorption onto the membranes or membrane filtration equipment. It is noted that Nghiem and Hawkes reported that adsorption is the main EDC and PPCPs removal mechanism for UF membranes and it was less important for NF and RO membranes.⁴⁴ It is noted that all the EDC and PPCPs contain electron donating functional group, such as primary amine, carboxylic acid, amide and phenolic hydroxyl. All the CSMM materials also contain charged end groups. As a result, there is a possibility of a charge transfer complex which improve the adsorption of EDC and PPCPs by the CSMMs modified PES membranes. In fact, based on the charge transfer complex the PEG₂₀₀-HBS should have better adsorption of EDC and PPCPs compared to other CSMMs, most probably PEG₂₀₀-HBS migrated to the membrane surface which easily formed the charge transfer complex with EDC and PPCPs during the filtration process.

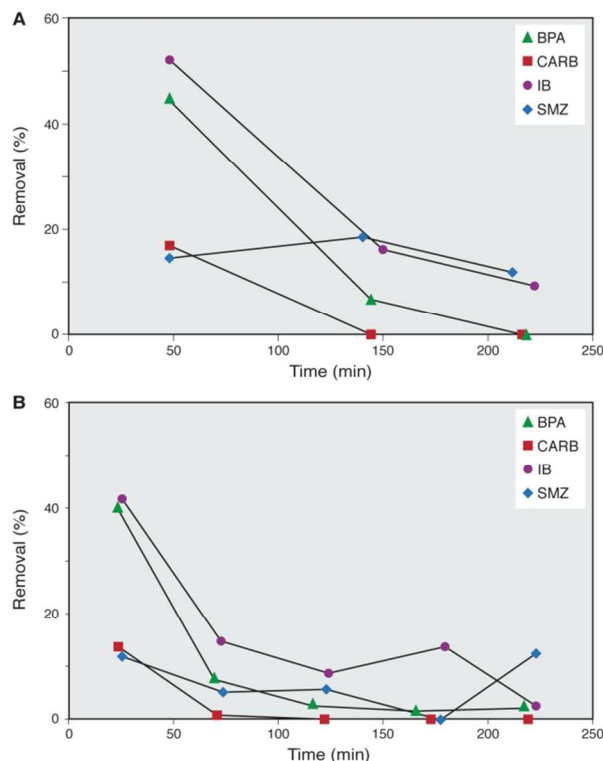


Fig. 11. Removal of EDC and PPCPs solutes for (A) PES18-0/PEG₂₀₀-HBS and (B) PES18-3/PEG₂₀₀-HBS membranes.

Conclusions

The modified PES membranes manufactured with the addition of CSMMs were slightly different than the control membranes; however, they were not very successful in removing the

Paper

target EDC and PPCPs from ultrapure water. There was an initial partial removal of the target compounds, but later samples showed no removal, which indicates that charge repulsion and size exclusion were not the controlling removal mechanism. The changes in membrane surface charge associated with the blending of the charged SMMs were relatively small compared to those observed in the literature, so the limited role of charge repulsion in the target compound removal is reasonable. The limited PPCP removal was not surprising since the tightest experimental membranes had a MWCO of approximately 10 kDa, while the target compounds had MWs in the 200 to 300 Dalton ranges, so size exclusion was not a factor. In light of this, future work on CSMMs should concentrate on nanofiltration applications.

The different CSMMs did have some impact on membrane characteristics and on membrane performance. There were no clear trends that were consistent for all the membrane preparation conditions (PES18-0, PES18-3 and PES20-0). In most cases, the CSMM did not significantly increase the charge of the PES membranes, however some of these additives increased the membrane flux, others decreased the MWCO and others increased the pore density. The PES18-3/PPG-HBC and PES20-0/PEG₄₀₀-HBS show significantly better fluxes than the controls because of their higher porosity. The different additives had an impact on the pore density, many increased it significantly. The charge introduced by the CSMMs was expected to produce more hydrophilic membranes; however, except for some membranes, the membrane CAs did not decrease. Comparison of the static CAs and surface charge of the PES20-0 membranes showed that the contact angles were controlled by variables other than surface charge. In light of their beneficial impact on fluxes and pore density, it is recommended that they be studied further.

Acknowledgements

Financial support from the Walkerton Clean Water Centre, Walkerton, ON, Canada; and the Ministry of the Environment, ON, Canada are gratefully appreciated. Partial financial support from the Natural Sciences and Engineering Research Council Canada is also gratefully acknowledged.

Notes and references

^a Dept. of Chemical and Biological Eng., University of Ottawa, 161 Louis Pasteur Pk., Ottawa, ON, K1N 6N5, Canada
Tel.: +1-613-562-5800 x 6085; fax: +1-613-562-5172.

E-mails: rana@uottawa.ca; rana@eng.uottawa.ca

^b Dept. of Civil Eng., University of Ottawa, 161 Louis Pasteur Pk., Ottawa, ON, K1N 6N5, Canada

^c Standards Development Branch, Ministry of the Environment, 40 St. Clair Ave. West, Toronto, ON, M4V 1M2, Canada

^d Walkerton Clean Water Centre, 220 Trillium Court, Walkerton, ON, N0G 2V0, Canada

[†] Present address: Industry Canada, Patent Branch - General Chemistry and Organic Division, 50 Victoria Street, Gatineau, QC, K1A 0C9, Canada

[‡] Present address: SJ Environmental Consultants (Windsor) Inc., 982 Grantham Ct., Windsor, ON, N9G 2S9, Canada

Electronic Supplementary Information (ESI) available: [Cross sectional diagram and photograph of the ultrafiltration cells, experimental set-up for streaming potential determination and diagram of zeta potential cell with holder]. See DOI: 10.1039/b000000x/

- 1 J.W. Birkett and J.N. Lester (Eds.), *Endocrine Disruptors in Wastewater and Sludge Treatment Processes*, Lewis Pub., Boca Raton, FL, 2003.
- 2 J.E. Drewes and L.S. Shore, Concerns about pharmaceuticals in water reuse, groundwater recharge, and animal waste. In: *Pharmaceuticals and Personal Care Products in the Environment*, Ch. Daughton and T.L. Jones-Lepp (Eds.), Am. Chem. Soc. Symp. Ser. 791, Washington, DC, 2001, pp. 206–228.
- 3 K. Kummerer (Ed.), *Pharmaceuticals in the Environment: Sources, Fate, Effects and Risks*, 3rd ed., Springer-Verlag, New York, NY, 2008.
- 4 N. Gilbert, *Nature*, 2011, **476**, 265.
- 5 A. Daneshvar, K. Aboulfadl, L. Viglino, R. Broséus, S. Sauvé, A.-S. Madoux-Humery, G.A. Weyhenmeyer and M. Prévost, *Chemosphere*, 2012, **88**, 131.
- 6 P.J. Ferguson, M.J. Bernot, J.C. Doll and T.E. Lauer, *Sci. Total Environ.*, 2013, **458–460**, 187.
- 7 J.E. Drewes, C. Bellona, M. Oedekoven, P. Xu, T.-U. Kim and G. Amy, *Environ. Prog.*, 2005, **24**, 400.
- 8 T. Heberer, *J. Hydrology*, 2002, **266**, 175.
- 9 K. Kimura, G. Amy, J.E. Drewes, T. Heberer and Y. Watanabe, *J. Membr. Sci.*, 2003, **227**, 113.
- 10 P.E. Stackelberg, E.T. Furlong, M.T. Meyer, S.D. Zaugg, A.K. Henderson and D.B. Reissman, *Sci. Total Environ.*, 2004, **329**, 99.
- 11 N.M. Vieno, H. Härkki, T. Tuhkanen and L. Kronberg, *Environ. Sci. Technol.*, 2007, **41** 5077.
- 12 A. Kumar and I. Xagorarakis, *Sci. Total Environ.*, 2010, **408**, 5972.
- 13 Y. Yoon, P. Westerhoff, S.A. Snyder and E.C. Wert, *J. Membr. Sci.*, 2006, **270**, 88.
- 14 L.D. Nghiem, A.I. Schäfer and M. Elimelech, *Environ. Sci. Technol.*, 2005, **39**, 7698.
- 15 S. Chang, T.D. Waite, A.I. Schäfer and A.G. Fane, *Environ. Sci. Technol.*, 2003, **37**, 3158.
- 16 V.A. Pham, J.P. Santerre, T. Matsuura and R.M. Narbaitz, *J. Appl. Polym. Sci.*, 1999, **73**, 1363.
- 17 D.E. Suk, G. Chowdhury, T. Matsuura, R.M. Narbaitz, J.P. Santerre, G. Pleizier and Y. Deslandes, *Macromolecules*, 2002, **35**, 3017.
- 18 D. Rana, T. Matsuura and R.M. Narbaitz, *J. Membr. Sci.*, 2006, **282**, 205.
- 19 D. Rana and T. Matsuura, *Chem. Rev.*, 2010, **110**, 2448.
- 20 Y. Kim, D. Rana, T. Matsuura and W.-J. Chung, *Chem. Commun.*, 2012, **48**, 693.
- 21 M.J. O'Neil, A. Smith, P.E. Heckelman, P.H. Dobbelaar, K.J. Roman, C.M. Kenney and L.S. Karaffa, (Eds.), *The Merck Index – An Encyclopedia of Chemicals, Drugs and Biologicals*. 15th Ed., Royal Society of Chemistry, Cambridge, UK, 2013.
- 22 T. Matsuura, *Synthetic Membranes and Membrane Separation Processes*, CRC Press, Boca Raton, FL, 1994.
- 23 D.B. Mosqueda-Jimenez, R.M. Narbaitz, T. Matsuura, G. Chowdhury, G. Pleizier and J.P. Santerre, *J. Membr. Sci.*, 2004, **231**, 209.
- 24 D.B. Mosqueda-Jimenez, R.M. Narbaitz and T. Matsuura, *J. Environ. Eng.*, 2004, **130**, 90.
- 25 S. Sourirajan, *Reverse Osmosis*, Academic Press, New York, NY, 1970, Ch. 1, p. 26.
- 26 S. Sourirajan and T. Matsuura, *Reverse Osmosis / Ultrafiltration Process Principles*, National Research Council Canada, Ottawa, ON, Canada, 1985, Ch. 7, p. 681.
- 27 A. Szymczyk, P. Fievet, M. Mullet, J.C. Reggiani and J. Pagetti, *J. Membr. Sci.*, 1998, **143**, 189.
- 28 M. Nyström, M. Lindström and E. Matthiasson, *Colloids Surf.*, 1989, **36**, 297.
- 29 H.T. Dang, Surface modifying macromolecules (SMM) incorporated ultrafiltration membranes for natural organic matter (NOM) removal: characterization and cleaning, Ph.D. Thesis, University of Ottawa, Ottawa-Carleton Institute of Environmental Engineering, Ottawa, ON, Canada, 2008.
- 30 H.T. Dang, R.M. Narbaitz and T. Matsuura, *J. Environ. Eng.*, 2010, **136**, 1161.
- 31 S. Singh, K.C. Khulbe, T. Matsuura and P. Ramamurthy, *J. Membr. Sci.*, 1998, **142**, 111.
- 32 W.M. Meylan, P.H. Howard, Eds., *Handbook of Physical Properties of Organic Chemicals*, CRC Press, Boca Raton, FL, 1997.
- 33 R.N. Wenzel, *J. Phys. Chem.*, 1949, **53**, 1466.
- 34 N. Bolong, A.F. Ismail, M.R. Salim, D. Rana, T. Matsuura and A. Tabe-Mohammadi, *Sep. Purif. Technol.*, 2010, **73**, 92.

Journal of Materials Chemistry A

Paper

- 35 Y. Kim, D. Rana, T. Matsuura, W.-J. Chung and K.C. Khulbe, *Sep. Purif. Technol.*, 2010, **72**, 123.
- 36 Y. Kim, D. Rana, T. Matsuura and W.-J. Chung, *J. Membr. Sci.*, 2009, **338**, 84.
- 37 C. Causserand, M. Nyström and P. Aimar, *J. Membr. Sci.*, 1994, **88**, 211.
- 38 M. Pontié, X. Chasseray, D. Lemordant and J.M. Lainé, *J. Membr. Sci.*, 1997, **129**, 125.
- 39 M.D. Afonso, *Desalination*, 2006, **191**, 262.
- 40 L. Zhang, G. Chowdhury, C.Y. Feng, T. Matsuura and R.M. Narbaitz, *J. Appl. Polym. Sci.*, 2003, **88**, 3132.
- 41 H.T. Dang, R.M. Narbaitz, T. Matsuura and K.C. Khulbe, *Water Quality Res. J. Canada*, 2006, **41**, 84.
- 42 D.B. Mosqueda-Jimenez, R.M. Narbaitz and T. Matsuura, *J. Appl. Polym. Sci.*, 2006, **99**, 2978.
- 43 A.I. Schäfer, I. Akanyeti and A.J.C. Semião, *Adv. Colloid Interface Sci.*, 2011, **164**, 100.
- 44 L.D. Nghiem and S. Hawkes, *Sep. Purif. Technol.*, 2007, **57**, 176.